ACCOUNTS
of chemical research

The Liquid–Liquid Interface as a Medium To Generate Nanocrystalline Films of Inorganic Materials

C. N. R. RAO* AND K. P. KALYANIKUTTY

Chemistry and Physics of Materials Unit, DST Nanoscience Unit, and CSIR Centre of Excellence in Chemistry, Jawaharlal Nehru Centre for Advanced Scientific Research, Jakkur P.O., Bangalore 560 064, India

RECEIVED ON AUGUST 31, 2007

CONSPECTUS

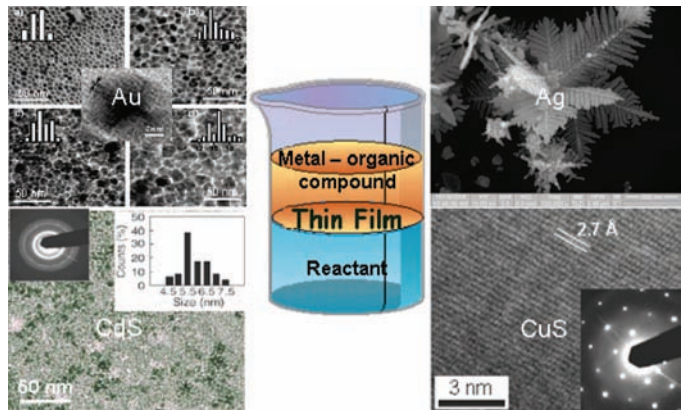

Unlike the air–water interface, the organic–aqueous (liquid–liquid) interface has not been exploited sufficiently for materials synthesis. In this Account, we demonstrate how ultrathin nanocrystalline films of metals such as gold and silver as well as of inorganic materials such as semiconducting metal chalcogenides (e.g., CdS, CuS, CdSe) and oxides are readily generated at the liquid–liquid interface. What is particularly noteworthy is that single-crystalline films of certain metal chalcogenides are also obtained by this method. The as-prepared gold films at the toluene–water interface comprise fairly monodisperse nanocrystals that are closely packed, the nature and properties of the films being influenced by various reaction parameters such as reaction temperature, time, reactant concentrations, mechanical vibrations, and the viscosity of the medium. The surface plasmon band of gold is markedly red-shifted in the films due to electronic coupling between the particles. The shift of the surface plasmon band of the Au film toward higher wavelengths with an accompanying increase in intensity as a function of reaction time marks the growth of the film. Depending on the reaction temperature, the Au films show interesting electrical transport properties. Films of metals such as gold are disintegrated by the addition of alkanethiols, the effectiveness depending on the alkane chain length, clearly evidenced by shifts of the surface plasmon bands. A time evolution study of the polycrystalline Au and CdS films as well as the single-crystalline CuS films is carried out by employing atomic force microscopy. X-ray reflectivity studies reveal the formation of a monolayer of capped clusters having 13 gold atoms each, arranged in a hexagonal manner at the toluene–water interface. The measurements also reveal an extremely small value of the interfacial tension. Besides describing features of such nanocrystalline films and their mode of formation, their rheological properties have been examined. Interfacial rheological studies show that the nanocrystalline film of Ag nanoparticles, the single-crystalline CuS film, and the multilayered CdS film exhibit a viscoelastic behavior strongly reminiscent of soft-glassy systems. Though both CuS and CdS films exhibit a finite yield stress under steady shear, the CdS films are found to rupture at high shear rates. An important advantage of the study of materials formed at the liquid–liquid interface is that it provides a means to investigate the interface itself. In addition, it enables one to obtain substrate-free single-crystalline films of materials.

Published on the Web 03/12/2008 www.pubs.acs.org/acr
10.1021/ar700192d CCC: $40.75

Introduction

Self-assembly, the process of formation of ordered aggregates, is a powerful strategy for creating novel structures of great academic interest as well as of technological value. Interfaces are an important means to generate two-dimensional self-assemblies of nanocrystals, providing a constrained environment for organized assembly. The air–water interface has been exploited for the preparation of films of metals and semiconductors, which have potential applications in nanodevices. For example, nanocrystal assemblies of gold have been prepared at the air–water interface by employing Langmuir–Blodgett (LB) technique.[1,2] Using a chloroform solution of $Au_{55}(PPh_3)_{12}Cl_6$, Schmid et al.[3] have self-assembled Au_{55} nanocrystals into monolayers in a LB trough. Somorjai and co-workers[4] have employed a LB trough to fabricate monolayers of monodisperse Rh nanocrystals on Si wafers as model 2D catalysts. Catalysts for the oxidation of formic acid have been prepared in the form of Langmuir layers of $Fe_{20}Pt_{80}$ nanoparticles.[5] Bawendi and co-workers[6] have prepared monolayers of monodisperse trioctylphosphine oxide capped CdSe quantum dots by the LB method. By exposing an LB film of lead stearate to H_2S, nanoparticles of PbS have been generated in the form of films.[7] LB films of iron oxide nanoparticles have been obtained by spreading a hexane suspension of oleic acid capped γ-Fe_2O_3 nanoparticles at the air–water interface.[8] Properties of thin films obtained by the LB technique are determined by the nature of the substrate as well as the reaction conditions, and the films are generally polycrystalline.

Unlike the air–water interface, the liquid–liquid (organic–aqueous) interface has not been investigated sufficiently, and it is only recently that there have been concerted efforts to understand the structure of the liquid–liquid interface. The liquid–liquid surface possesses unique thermodynamic properties such as viscosity and density. A liquid–liquid interface is a nonhomogeneous region having a thickness on the order of a few nanometers. The interface is not sharp, since there is always a little solubility of one phase in the other. One of the problems that has been studied in detail at the liquid–liquid interface relates to interfacial charge transfer reactions and dynamics.[9] Distribution of ions and solvent molecules, which determines the structure of a liquid–liquid interface, has recently been investigated by Schlossman and co-workers.[10] Using X-ray reflectivity and molecular dynamics simulations, these workers find that ion sizes and ion–solvent interactions affect the ion distributions near the interface. The relevance of the liquid–liquid interface has been noted in some other areas such as environmental chemistry, cell biology, and catalysis. The interface between two immiscible liquids offers an important alternative path for the self-assembly and chemical manipulation of nanocrystals.[11] Nanoparticles are highly mobile at the interface and rapidly achieve an equilibrium assembly by reduction in interfacial energy. The three parameters that have been found to influence the energy of the assembly process at the liquid–liquid interface are (i) the nature of the interface, (ii) surface modification of the nanoparticles at the interface, and (iii) the effective radius of the nanoparticles, smaller nanoparticles adsorbing more weakly to the interface than larger ones. Binks and Clint[12] have theoretically treated the wetting of silica particles in terms of the surface energies at the oil–water interface to interpret the interactions between the solid and the liquid phases and to predict the oil–water contact angles for a solid of given hydrophobicity. Only if the contact angle is exactly 90° will the particle be located at the middle of the oil–water interface.

Russel and co-workers[13] have investigated the assembly of phosphine oxide functionalized CdSe nanoparticles of two different diameters by competitive adsorption at the toluene–water interface by employing fluorescence spectroscopy. Benkoski et al.[14] have developed the so-called fossilized liquid assembly for the creation of 2-D assemblies from nanoscale building blocks. By investigating the interactions of a variety of particles such as uncharged, charged, functionalized, and nonfunctionalized, deposited at dodecanediol dimethacrylate/water interface, they have shown that nanoparticles aggregate into a wide variety of complex morphologies. These results provide evidence for the importance of asymmetric dipole interaction in generating the complex morphologies. There are a few assorted reports in the literature where the liquid–liquid interface or a mixture of immiscible liquids has been used for the synthesis or crystallization of nanostructures and other materials. The Brust method,[15] which has been widely employed for the preparation of Au nanocrystals by the reduction of $AuCl_4^-$ by $NaBH_4$ in the presence of an alkanethiol, is carried out in a water–toluene mixture in the presence of a phase-transfer reagent such as tetraoctylammonium bromide. Stucky and co-workers[16] have prepared mesoporous fibers of silica by treating the silica precursor dissolved in an organic phase such as hexane, toluene, or CCl_4 with surfactant molecules dissolved in the aqueous phase. CdS nanoparticles in the form of LB films have been prepared by reacting an aqueous $CdCO_3$ solution with CS_2 in CCl_4.[17] Monodisperse, luminescent nanocrystals of CdS have been prepared by mixing a solution of cadmium–myristic acid and *n*-triphenylphosphine oxide in toluene with

an aqueous solution of thiourea, followed by heating under stirring.[18] Langmuir films of silver nanoparticles have been prepared at the water−dichloromethane interface.[19] With Pickering emulsions as a template, dodecanethiol-capped Ag nanoparticles have been self-assembled at the trichloroethylene−water interface.[20] Song et al.[21] have employed the butanol−water interface for the crystallization of Se nanorods. Amorphous Se nanoparticles were first prepared in the aqueous medium and then transported to the butanol−water interface using polyvinylpyrrolidone (PVP), to obtain crystalline nanorods of Se. Cheetham and co-workers[22] have employed a cyclohexanol−water mixture to prepare single crystals of copper adipate. Although the assembly of pregenerated nanoparticles at liquid–liquid interfaces has been examined to some extent, this interface has not been exploited for the synthesis of nanoparticles and their assemblies.

In this Account, we describe a simple but elegant means of generating ultrathin nanocrystalline films of various materials at the organic−aqueous interface. The method primarily involves taking a metal organic compound in the organic layer and a reducing, a sulfiding, or an oxidizing agent in the aqueous layer. The reaction occurs at the interface giving rise to a film at the interface with several interesting features. We describe nanocrystalline films of gold in detail to show how the various reaction parameters affect the films formed at the interface and how alkanethiols bring about the disintegration of the films. We also demonstrate the power of the method in generating ultrathin polycrystalline, as well as single-crystalline, films of some metal chalcogenides at the interface. The formation of single-crystalline films is indeed a noteworthy feature. We believe that this method can be adopted not only for generating nanocrystalline films of various materials but also to study processes occurring at the liquid–liquid interface.

General Experimental Procedure

Use of the liquid–liquid interface for preparing materials in the form of nanocrystalline films is simple and straightforward.[1a,23]The procedure to prepare nanocrystalline films of metals involves taking a metal organic precursor in the organic layer and then injecting an appropriate reducing agent into the aqueous layer to obtain a film comprising metal nanocrystals. In order to prepare nanocrystalline films of metal sulfides, Na_2S is used as the source of sulfur, while Na_2Se or *N*,*N*-dimethylselenourea is used as the source of selenium to prepare films of metal selenides.

We shall illustrate the method of preparation of nanocrystalline films with two examples. To prepare nanocrystalline gold films, $Au(PPh_3)Cl$ (Ph = phenyl) is found to be a good precursor. In a typical preparation, 10 mL of a 1.5 mM solution of $Au(PPh_3)Cl$ in toluene is allowed to stand in contact with 16 mL of a 3.25 mM solution of NaOH in water in a 100 mL beaker at 300 K. Tetrakishydroxymethylphosphonium chloride (THPC; 300 μL of 50 mM), which acts as the reducing agent,[23a] is slowly injected to the aqueous layer with minimal disturbance to the organic layer. A slight pink coloration of the interface indicates the onset of reduction of the gold salt. As the reaction proceeds, the color of the interface intensifies, finally resulting in a robust film at the interface as shown in Figure 1a. For preparing a nanocrystalline film of CdS, 0.0045 g of Na_2S is dissolved in 30 mL of water (2 mM) in a 100 mL beaker, and 0.0125 g of cadmium cupferronate [$Cd(cup)_2$] is dissolved in 30 mL of toluene (1 mM) by ultrasonication. A few drops of *n*-octylamine are added to the $Cd(cup)_2$ solution in order to make it completely soluble. The toluene solution is slowly added to the aqueous Na_2S solution in a 100 mL beaker at 30 °C. The interface attains a yellow color within a few minutes, and a distinct film is formed after 10 h. In Figure 1b, we show a nanocrystalline film of CdS, so formed.

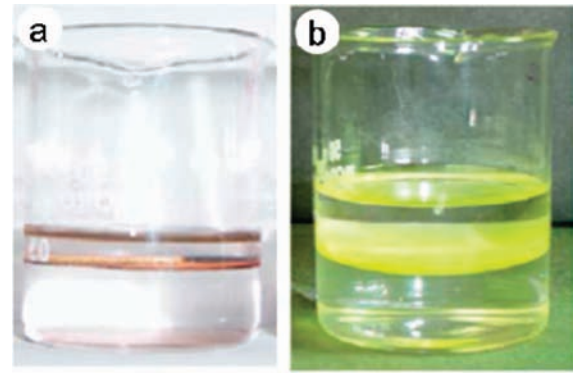

FIGURE 1. Nanocrystalline films of (a) Au and (b) CdS formed at the toluene−water interface.

Gold and Other Metals

We shall discuss ultrathin films of gold nanocrystals in some detail to illustrate the features of the method as well as the interesting features of the materials obtained by this method. As-prepared Au films, obtained at 30 °C after 24 h of the reaction at the toluene−water interface comprise fairly monodisperse nanoparticles with a mean diameter of ~7 nm (see the TEM image given in Figure 2a). The nanocrystals are closely packed with a typical interparticle distance of ~1 nm. Furthermore, they are single-crystalline as revealed by the high-resolution electron microscope (HREM) image given as an inset in Figure 2. The image shows the (111) planes of gold, sepa-

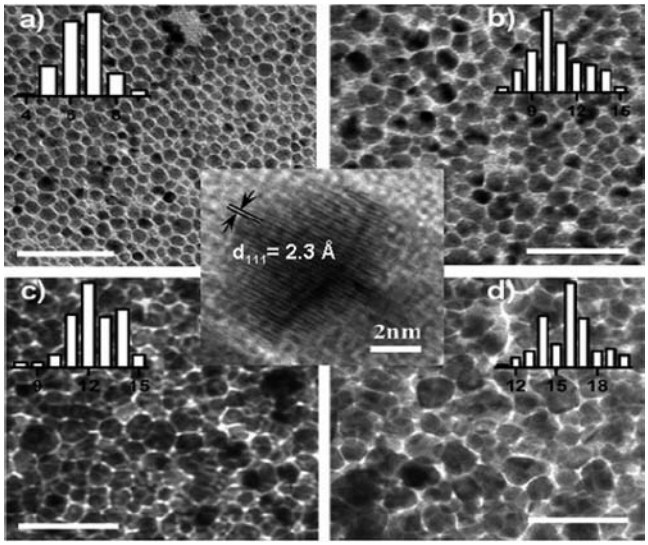

FIGURE 2. TEM images of the ultrathin nanocrystalline Au films obtained at the liquid–liquid interface after 24 h at (a) 30, (b) 45, (c) 60, and (d) 75 °C. Histograms of particle size distribution are shown as insets. The scale bars correspond to 50 nm. A high-resolution image of an individual particle is shown at the center. Reproduced from ref 24. Copyright 2005 American Chemical Society.

rated by a distance of ~2.3 Å. Such nanocrystalline films could also be obtained by using other solvent pairs such as CCl_4–water and butanol–water. Reaction parameters such as the temperature, reaction time, concentrations of the metal precursor and the reducing agent, and the viscosity of the aqueous layer affect the nature and properties of the nanocrystalline films.

The effect of temperature on the size distribution of the Au nanocrystals can be readily seen from the TEM images in Figure 2. The mean diameters of the nanocrystals formed at 30, 45, 60, and 75 °C are 7, 10, 12, and 15 nm, respectively, but the interparticle separation remains nearly the same at ~1 nm. X-ray diffraction measurements show that with increase in temperature, the crystallinity of the film increases (Figure 3). The films obtained at 45 and 60 °C exhibit prominent (111) peaks (d = 2.33 Å), while those obtained at 30 °C show weak reflections, probably due to the small particle size. The growth of the (111) peak with temperature indicates an increase in the particle size.

Increasing the concentration of the metal precursor yields nanocrystalline films with a larger number of particles, but the size distribution is essentially unaffected. The thickness of the film also increases with the increase in the metal precursor concentration. The use of high concentrations of the reducing agent results in less uniform films with altered distributions in the nanoparticle diameter. A slight increase in the size of the Au nanoparticles was observed when the viscosity of the aqueous layer was increased by the addition of glycerol.

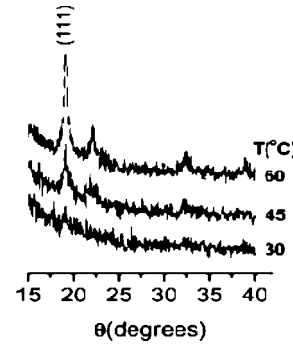

FIGURE 3. X-ray diffraction patterns of nanocrystalline Au films obtained at different temperatures. Reproduced from ref 24. Copyright 2005 American Chemical Society.

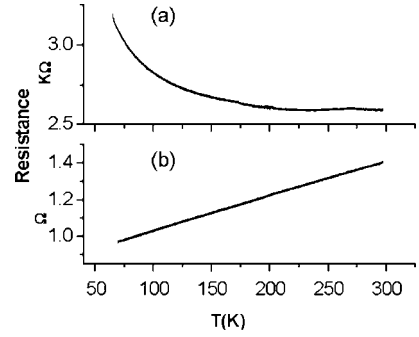

FIGURE 4. Temperature variation of the electrical resistance of the Au films prepared at (a) 45 and (b) 60 °C (current used, 10 mA). Modified from ref 24. Copyright 2005 American Chemical Society.

Reactions at the interface carried out on a vibration-free table yielded nanocrystalline films with reduced roughness, comprising particles of smaller size.

The Au films formed at the interface show interesting electrical transport properties that are dependent on the reaction temperature (see Figure 4).[24] Four-probe electrical resistance measurements on the nanocrystalline films show a metal to insulator transition, metallic behavior being shown by the films formed at high temperatures (>45 °C). The films formed at lower temperatures (≤45 °C) show insulating behavior.

Atomic force microscopy (AFM) shows the thickness of the films to be in the 40–140 nm range. The contact mode AFM image in Figure 5a shows the boundary of a Au film on a mica substrate. The height profile of the film in Figure 5b gives an estimate of the thickness to be ~60 nm. AFM images covering a few micrometers yield a root-mean-square roughness in the range 30–35 nm.

The growth of Au films could be followed as a function of reaction time by UV–visible absorption spectroscopy (Figure 6). The Au plasmon band gets red-shifted due to the increase in the electronic coupling between the particles, accompanied by an increase in the intensity. The absorption band shows

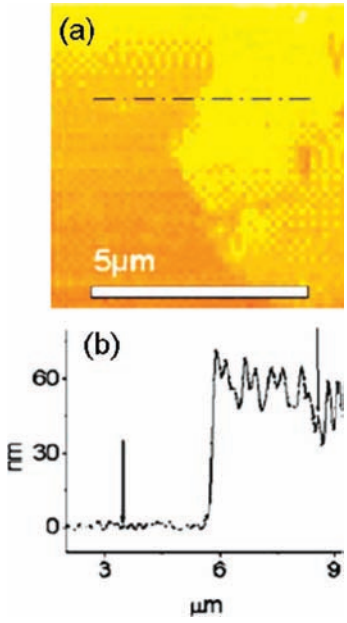

FIGURE 5. (a) Contact-mode AFM image showing the boundary of Au film on a mica substrate and (b) the *z*-profile. Reproduced from ref 24. Copyright 2005 American Chemical Society.

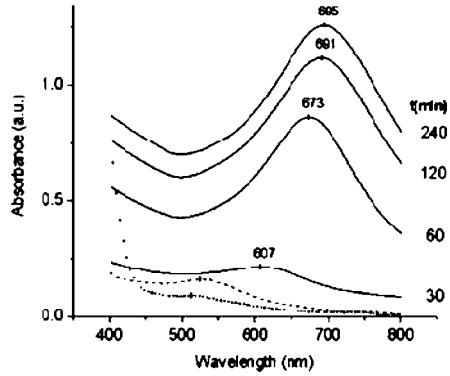

FIGURE 6. Evolution of the electronic absorption spectra with the growth of the nanocrystalline Au film at the interface at 45 °C (full curves) and spectra of octylamine-capped Au nanocrystals in toluene (broken line) and mercaptoundecanoic acid-capped nanocrystals in water (dotted line). Modified from ref 24. Copyright 2005 American Chemical Society.

negligible change after 120 min. At this stage, the films presumably consist of well-packed nanocrystals.

The effect of surfactants such as tetraoctylammonium bromide (TOAB) and cetyltrimethylammonium bromide (CTAB) on the nanostructures formed when the gold ions present in the organic phase are reduced at the interface by hydrazine (in the aqueous phase) has been investigated.[25] The surfactants give rise to extended fractal networks with a fractal dimension of 1.7 at the interface (Figure 7a). The fractals themselves comprise cauliflower-like spherical units (see top inset in Figure 7a) formed of pentagonal nanorods.

Till now, we have been examining the formation of uniform and robust nanocrystalline films of Au. The films, once

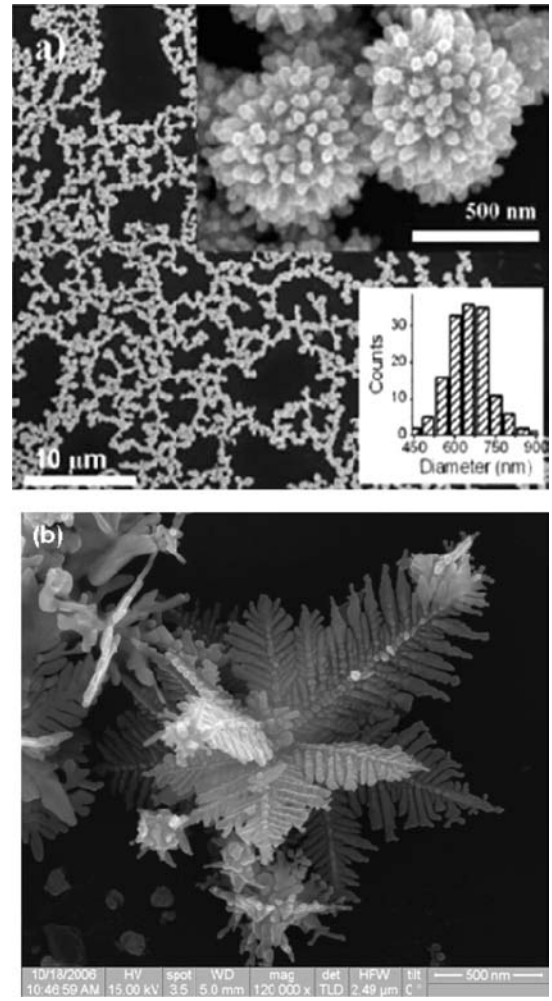

FIGURE 7. Panel a shows an SEM image of the fractal network formed by cauliflower-like gold structures by employing TOAB. The inset on the top right corner shows a high-resolution image of the cauliflower-like structures. The inset at the bottom shows the histogram of the size distribution of cauliflower-like structures. Panel b shows a dendritic nanostructure of Ag. Reproduced with permission from ref 25. Copyright 2008 Elsevier.

formed, can be disintegrated or disordered by the addition of *n*-alkanethiols.[24,26] Addition of alkanethiols is accompanied by a progressive blue shift of the plasmon absorption band of the film, suggesting that the electronic coupling between the nanocrystals gets reduced due to the increased separation between the nanocrystals. Figure 8a shows the variation in the shift of the absorption band brought about by the addition of hexadecanethiol. Interaction with thiols also brings about a change in the morphology of the film as shown in the adjoining AFM images. By varying the chain length of the alkanethiol, one is actually varying the distance between the nanoparticles, thereby giving rise to a blue shift proportional to the length of the alkane chain (Figure 8b). The rate of disordering or disintegration of the Au films is also affected by the chain length of the alkanethiols; the longer the chain

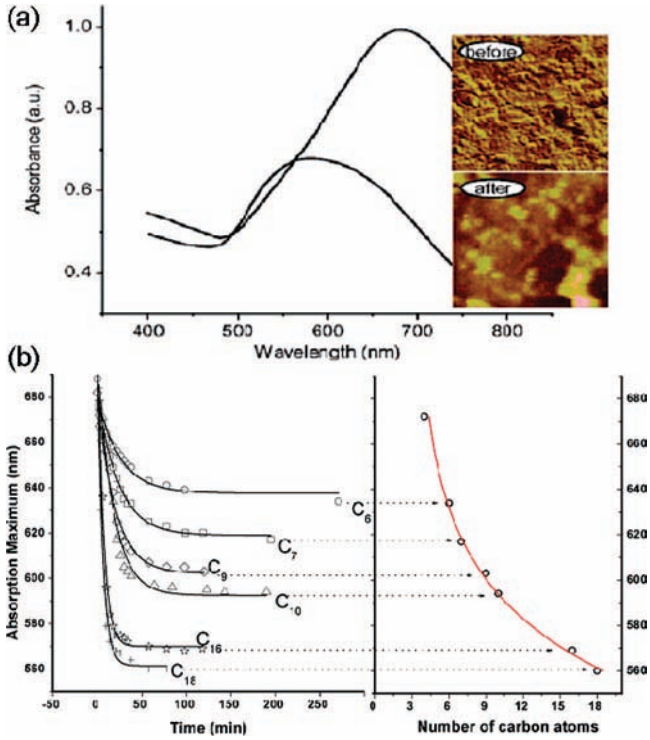

FIGURE 8. Panel a shows the electronic absorption spectra of a Au film before and after treatment with hexadecanethiol solution for 6 h. Tapping mode AFM images are shown alongside (scan area 500 nm × 500 nm). Reproduced from ref 24. Copyright 2005 American Chemical Society. (b) Time variation of the absorption maximum of Au nanocrystalline films on interaction with alkanethiols of different chain lengths (left) and variation in the limiting absorption maximum with chain length of the thiol adsorbed (right). Reproduced from ref 26. Copyright 2008 American Chemical Society.

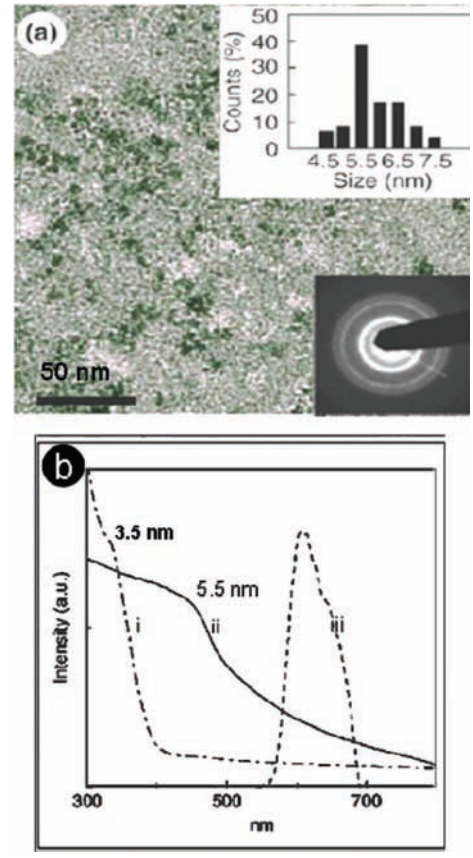

FIGURE 9. Panel a shows the TEM image of 5.5 nm CdS nanocrystals obtained at room temperature at the interface. Insets give the SAED pattern and the particle size distribution. Panel b shows the UV–visible absorption spectra of (i) 3.4 nm and (ii) 5.5 nm CdS nanocrystals and (iii) the photoluminescence spectrum of 5.5 nm CdS nanocrystals. Modified with permission from ref 28. Copyright 2003 Elsevier.

length, the faster is the rate. Calorimetric measurements also lend evidence for such a process.

It has also been possible to obtain nanocrystalline films of other metals such as Ag, Pd, and Cu at the toluene–water interface by taking $Ag_2(PPh_3)_4$, palladium acetate, and $Cu(PPh_3)Cl$, respectively, in the organic layer.[23] By carrying out the reaction in the presence of TOAB, we have obtained dendritic structures of Ag (Figure 7b).[25] By taking mixtures of the corresponding metal precursors in the organic layer, we have prepared nanocrystalline films of binary Au–Ag and Au–Cu alloys and ternary Au–Ag–Cu alloys.[27]

Metal Chalcogenides

Ultrathin films of metal sulfides such as CdS, CuS, ZnS, and PbS are obtained at the organic–aqueous interface by the reaction of Na_2S in the aqueous layer with the corresponding metal cupferronate in the organic layer.[28–30] We show typical results in the case of CdS. TEM images reveal the films to be composed of nanocrystals of 5.5 nm diameter (Figure 9a). The powder XRD pattern of the film shows that the CdS nanocrystals crystallize in the rock-salt structure rather than in the wurtzite structure. Increasing the reaction temperature and the concentration of the reactants yields bigger nanocrystals. When the viscosity of the aqueous medium is doubled by the addition of glycerol, the size of the nanocrystals is reduced to 3.5 nm. The UV–vis absorption spectrum of the nanocrystals (Figure 9b) shows a broad absorption maximum, which is blue-shifted compared with the bulk CdS due to quantum confinement. The PL spectrum of the 5.5 nm particles shows a peak at 610 nm.

Polycrystalline thin films of CdSe have been prepared at the organic–water interface by reacting cadmium cupferronate in the toluene layer with dimethylselenourea in the aqueous layer.[31] XRD measurements confirm the formation of cubic CdSe at the interface. TEM images reveal the films to be made up of nanocrystals with diameters ranging from 8 to 20 nm (Figure 10a). Time-dependent growth of the CdSe film at 20 °C has been examined by UV–vis absorption spectroscopy. All

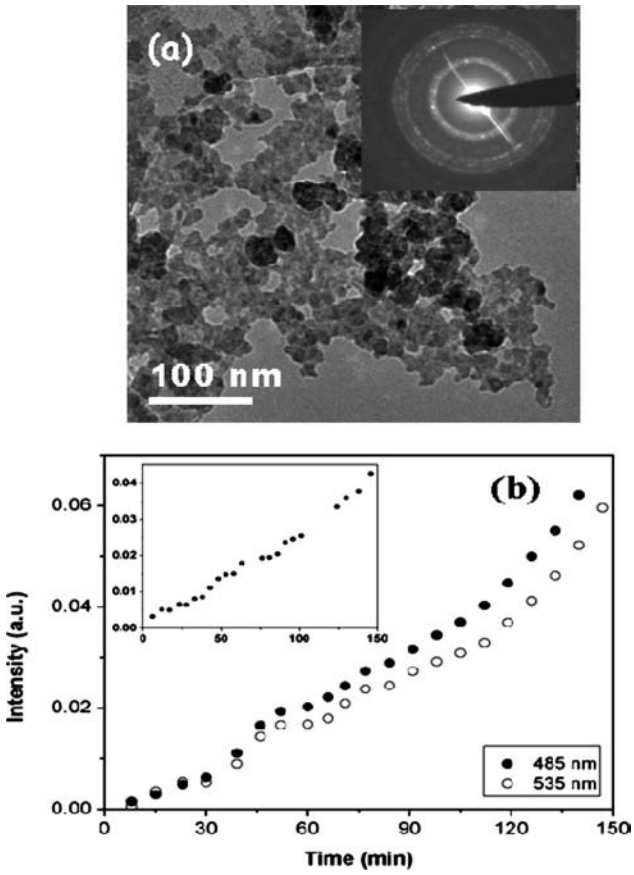

FIGURE 10. (a) TEM image of a CdSe film showing particles obtained by reacting aqueous solution of DMSU at 30 °C and (b) a plot showing the time-dependent growth of the absorption bands at two different wavelengths. Reproduced with permission from ref 31. Copyright 2007 American Scientific Publishers.

the films, including the one obtained after 3 min of the reaction, showed an absorption onset around 700 nm corresponding to the bulk band gap of CdSe and two higher order absorption bands at 485 and 535 nm. With increase in reaction time, the spectra indeed grew in intensity, without any appreciable shift in the positions of the band edge or the absorption bands, suggesting that CdSe nanoparticles possessing a size beyond the quantum confinement effects are formed at the interface within the first few minutes. Accordingly, the intensity versus time plots for the 485 and 535 nm bands, in Figure 10b, show a monotonic increase.

What is truly noteworthy is that we have been able to get single-crystalline films of some of the metal chalcogenides at the interface. In the case of CuS, we obtain continuous films, extending over wide areas (Figure 11a). A HREM image showing the (006) planes of hexagonal CuS and the corresponding SAED pattern given in Figure 11b reveal the single-crystalline and essentially defect-free nature of the CuS films. The thickness of the film was estimated to be ~50 nm from AFM and ellipsometric studies. In Figure 11c, we show a HREM

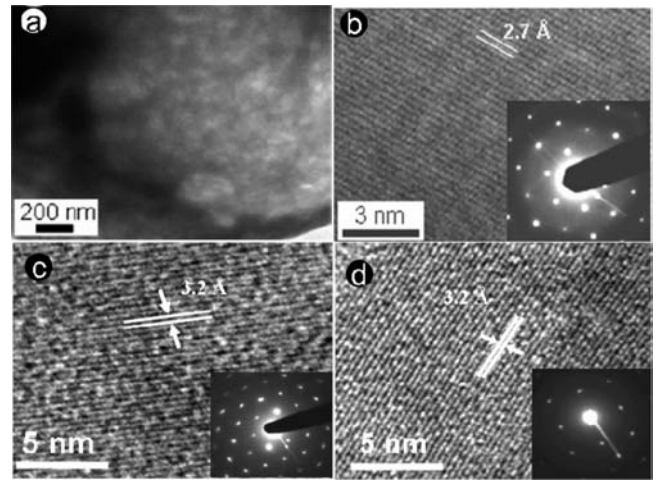

FIGURE 11. (a) TEM image of a CuS film, (b) HREM and SAED pattern of the film shown in panel a (Reproduced from ref 29. Copyright 2004 American Chemical Society), and HREM images and SAED patterns of (c) ZnS film and (d) PbS film (Reproduced with permission from ref 30. Copyright 2006 Elsevier).

image of a single-crystalline ZnS film. The (100) planes, separated by a distance of 3.2 Å, as seen in the HREM image correspond to hexagonal ZnS. The Bragg spots in the SAED pattern conform to the 0001 zone axis of hexagonal ZnS. In Figure 11d, we show the HREM image and the SAED pattern of a PbS film generated at the interface to reveal the single-crystalline nature. The HREM image gives a separation of 3.2 Å, corresponding to the separation between the (100) planes of cubic PbS. Single-crystalline CuSe thin films have also been obtained at the interface. Apart from single-crystalline films of metal sulfides, we could obtain metal sulfide bilayers such as CuS−CdS, CuS−PbS, and CdS−PbS at the toluene−water interface by employing the respective metal cupferronates.

Metal Oxides

By reacting $Cu(cup)_2$ in the organic layer with an aqueous NaOH solution, one obtains single-crystalline films of monoclinic CuO at the organic−aqueous interface at 70 °C.[29] It has been possible to obtain crystalline films of ZnO by the reaction of $Zn(cup)_2$ in toluene with an aqueous solution of NaOH at 25 °C.

Mode of Growth of the Films at the Interface

A time evolution study of Au films by AFM shows that just after 10 min of the reaction, a film made up of nanocrystals of size ~5−7 nm is formed. Although the size of the nanoparticles remains nearly the same even after 180 min of the reaction, we have found some evidence for the aggregation of nanoparticles in the films. The organic capped nanocrys-

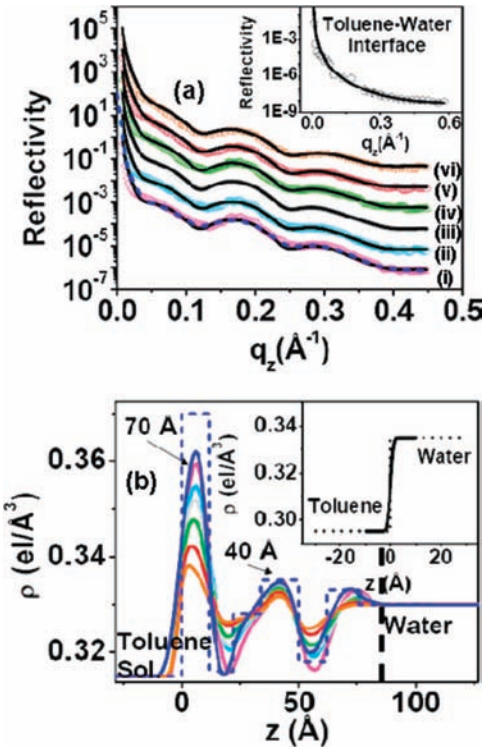

FIGURE 12. Reflectivity curves collected after initiation of the reaction (i, 194; ii, 224; iii, 253; iv, 283; v, 312; vi, 364 min) and the fits (solid line) and (b) extracted electron density profiles for the six reflectivity curves (i–vi) given in panel a as a function of depth. A simple model without (dashed line) and with roughness convolution (solid line) is also shown. The insets in panels a and b show the reflectivity data and the EDPs, respectively, of the bare toluene–water interface and the corresponding fit (solid line). Taken from ref 32.

tals form an ordered arrangement giving rise to large features in the AFM images. The appearance of such large features makes it difficult to carry out a proper AFM study of the Au films. However, the AFM study shows that the thickness of the films increases progressively with time.

The formation of Au nanoparticle films has been investigated by X-ray reflectivity and diffuse scattering employing synchrotron radiation.[32] The oscillations in the reflectivity curves, collected after the initiation of the reaction (see Figure 12a), indicate the presence of a thin film at the toluene–water interface. The extracted final electron density profiles (EDPs; Figure 12b) from the reflectivity curves show three layers of gold clusters at 70 Å, 40 Å, and just above the water surface with central electron density values of 0.37, 0.33, and 0.33 electrons Å^{-3}. The layers have a vertical separation of 30 Å, the electron density between these layers corresponding to that of a typical organic material. A preliminary study shows that small Au nanoparticles covered by organic coatings form hexagonal clusters at the toluene–water interface (Figure 13). Each cluster consists of 13 nanoparticles of

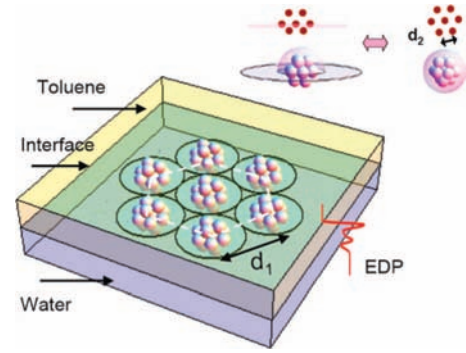

FIGURE 13. Schematic showing the hexagonal arrangement of organic-capped Au nanocrystals at the toluene–water interface. Taken from ref 32.

diameter ~12 Å with an organic capping of ~11 Å. Diffuse scattering measurements give a small value of interfacial tension, indicating an enhancement in the interfacial roughness caused by the presence of an organic layer at the interface.

The growth of the CdS polycrystalline thin films at the organic–aqueous interface has been studied as a function of time by employing AFM. The CdS film obtained after 30 min is made up of nanoparticles of diameter in the range ~5–7 nm. Nanoparticle aggregates of size in the range 80–200 nm are seen on the surface of the film. After 60 min of the reaction, the vertical growth of the aggregates saturates. The nanoparticles constituting the aggregates spread out laterally, thus reducing the overall thickness of the sample. With time, the aggregates gradually self-assemble to form a close-packed layer.

The growth of single-crystalline CuS films has also been examined as a function of reaction time by employing AFM. Nanoparticles of diameter in the range 7–8 nm are found to constitute the films. The amplitude image of the 30 min sample (Figure 14a) shows the presence of nanoparticle aggregates of size mainly in the range 50–100 nm. As the reaction proceeds, the initially formed nanoparticle aggregates come closer to each other and pack themselves at the interface to give flakes or uneven pieces of CuS within 50 min of reaction (denoted by arrows in Figure 14b). In the next 15 min of the reaction, the flakes coalesce to give a continuous and extended film at the interface. The process of formation of flakes and their coalescence repeats, giving rise to a thick film at the interface at the end of 180 min of the reaction (Figure 14c). Here we could hardly observe any individual nanoparticles. This is in contrast to the Au and CdS films, where the individual nanoparticles remained.

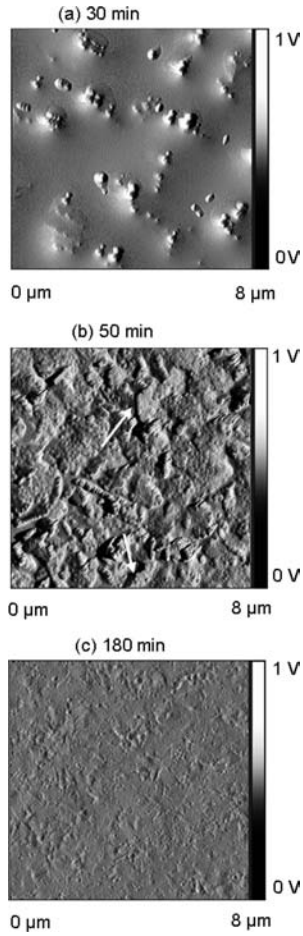

FIGURE 14. Tapping mode AFM images (amplitude channel) of CuS films grown at the toluene–water interface for (a) 30 min and (b) 50 min and (c) contact mode image obtained from the deflection channel of the film grown for 180 min.

Rheological Properties of the Films

Interfacial properties of Ag nanoparticles formed at the toluene–water interface have been investigated by using a biconal bob interfacial rheometer.[33] Strain amplitude measurements carried out on the film reveal a shear-thickening peak in the loss moduli (G'') at large amplitudes, followed by a power law decay of storage (G') and loss moduli with exponents in the ratio 2:1 (see Figure 15a). In the frequency sweep measurements carried out at low frequencies, G' remains nearly independent of the frequency over the range of frequencies probed, whereas G'' shows a power law dependence with a negative slope (Figure 15b). Such a low-frequency response of the 2D film of metal nanoparticles is reminiscent of a soft glassy system with long structural relaxation times. Steady shear measurements carried out on the film revealing a finite yield stress as the shear rate goes to zero, along with a significant deviation from the Cox–Merz rule, confirm that the monolayer of Ag nanoparticles at the interface forms a soft two-dimensional colloidal glass.

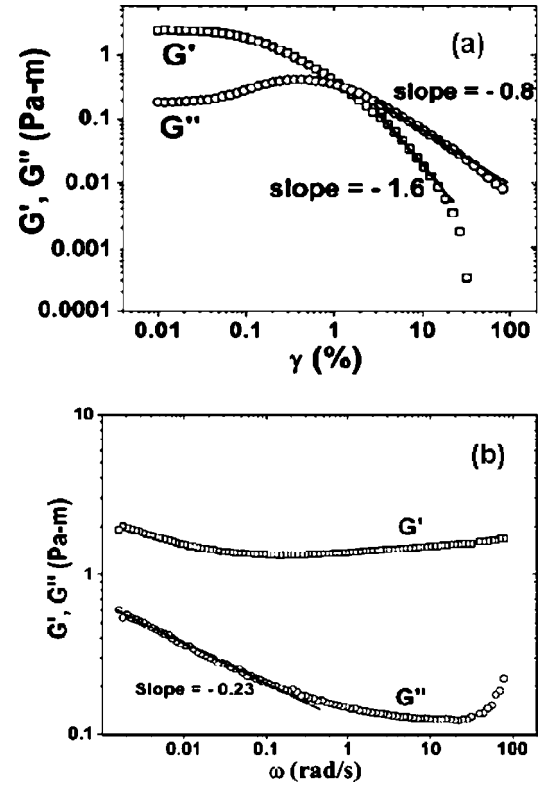

FIGURE 15. Panel a shows the strain amplitude sweep experiment on the 2D film of Ag nanoparticles. The storage modulus, G' (□), is higher than the loss modulus, G'' (○) at low strain amplitudes. Panel b shows the frequency dependence of interfacial storage, G' (□), and loss, G'' (○), moduli of the film. Reproduced from ref 33. Copyright 2007 American Chemical Society.

Interfacial rheological measurements carried out on nanocrystalline films of CdS, as well as on single-crystalline films of CuS, indicate a distinct nonlinear viscoelastic behavior for the films under oscillatory shear.[34] A smooth multilayered CdS film formed at higher concentrations and the single-crystalline CuS film exhibit distinct peaks in the loss modulus above a critical strain amplitude, followed by a power law decay of G' and G'' at higher strain amplitudes, with the decay exponents in the ratio 2:1 (Figure 16). The frequency sweep response of both films, exhibiting a solid-like behavior over the range of angular frequencies probed, is similar to that of the Ag film, a characteristic feature of soft glassy systems. However, the mesoporous CdS film formed at low concentrations, where the pore boundaries form a surface fractal with a fractal dimension of 2.5, exhibits a monotonic decay of storage and loss modulus at large strain amplitudes. Under steady shear, compared with the CuS film, the finite yield stress exhibited by the CdS film is a magnitude lower, and the film is found to rupture under steady shear or at high strain amplitudes.

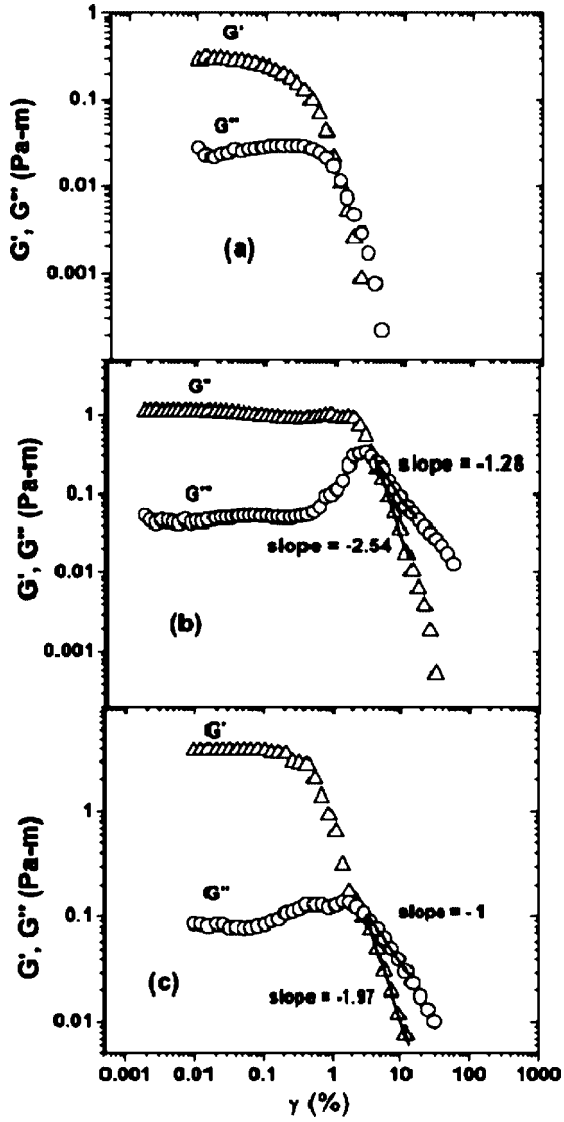

FIGURE 16. Strain amplitude sweep measurements on (a) CdS (low reactant concentrations), (b) CdS (high reactant concentrations), and (c) nanofilms formed at the toluene–water interface at 22 °C. Reproduced from ref 34. Copyright 2008 Elsevier.

Conclusions

This Account should clearly bring out how the liquid–liquid interface can be exploited to prepare nanocrystalline films of various materials with wide ranging properties. What is noteworthy is that all the films are ultrathin with the thickness ranging from 40 to 100 nm. Furthermore, the method enables one to obtain substrate-free films, some of which are single-crystalline. It must be noted that obtaining single-crystalline films is difficult by any other physical or chemical method. The films prepared at the interface can be readily transferred to any substrate. By employing the organic–aqueous interface, one can prepare interesting films of inorganic materials with hydrophilic and hydrophobic coatings on opposite sides. It should also be possible to obtain bilayers of materials at the interface. Preliminary experiments show that CuS–CdS, CuS–PbS, and CdS–PbS bilayers can be prepared at the interface. The study of films of materials at the liquid–liquid interface will also provide a means to understand the nature of the interface itself.

The authors thank their colleagues, Prof. G. U. Kulkarni, Dr. U. K. Gautam, Dr. M. Ghosh, and V. V. Agrawal, who have collaborated on some aspects of the films at the liquid–liquid interface.

BIOGRAPHICAL INFORMATION

C. N. R. Rao is National Research Professor of India, Linus Pauling Research Professor at the Jawaharlal Nehru Centre for Advanced Scientific Research (JNCASR), and Honorary Professor at the Indian Institute of Science, Bangalore. He is a member of many academies including the Royal Society and the U.S. National Academy of Sciences. His main research interests are in solid state and materials chemistry, in which area he has published over 1000 research papers and 30 books. He is the recipient of the Dan David Prize for Materials Research.

K. P. Kalyanikutty received her B.Sc. degree from the Univeristy of Calicut and M.S. degree from JNCASR. She is continuing work for her Ph.D. degree in the area of nanomaterials.

FOOTNOTES

*Corresponding author. Fax: 00 91 80 2208 2766. E-mail: cnrrao@jncasr.ac.in.

REFERENCES

1 (a) Petty, M. C. *Langmuir-Blodgett films: An introduction*; Cambridge University Press: Cambridge, U.K., 1996. (b) Gelbart, W. M.; Sear, R. P.; Heath, J. R.; Chaney, S. Array Formation in Nano-colloids: Theory and Experiment in 2D. *Faraday Discuss.* **1999**, *112*, 299–307. (c) Rao, C. N. R.; Agrawal, V. V.; Biswas, K.; Gautam, U. K.; Ghosh, M.; Govindaraj, A.; Kulkarni, G. U.; Kalyanikutty, K. P.; Sardar, K.; Vivekchand, S. R.C. Soft Chemical Approaches to Inorganic Nanostructures. *Pure Appl. Chem.* **2006**, *78*, 1619–1650.

2 Mayya, K. S.; Patil, V.; Sastry, M. Lamellar Multilayer Gold Cluster Films Deposited by the Langmuir–Blodgett Technique. *Langmuir* **1997**, *13*, 2575–2577.

3 Schmid, G.; Baumle, M.; Beyer, N. Ordered Two-Dimensional Monolayers of Au_{55} Clusters. *Angew. Chem., Int. Ed.* **2000**, *39*, 181–183.

4 Zhang, Y.; Grass, M. E.; Habas, S. E.; Tao, F.; Zhang, T.; Yang, P.; Somorjai, G. A. One-step Polyol Synthesis and Langmuir–Blodgett Monolayer Formation of Size-Tunable Monodisperse Rhodium Nanocrystals with Catalytically Active (111) Surface Structures. *J. Phys. Chem. C* **2007**, *111*, 12243–12253.

5 Chen, W.; Kim, J.; Xu, L-P.; Sun, S.; Chen, S. Langmuir–Blodgett Thin Films of $Fe_{20}Pt_{80}$ Nanoparticles for the Electrocatalytic Oxidation of Formic Acid. *J. Phys. Chem. C* **2007**, *111*, 13452–13459.

6 Dabbousi, B. O.; Murray, C. B.; Rubner, M. F.; Bawendi, M. G. Langmuir–Blodgett Manipulation of Size-Selected CdSe Nanocrystallites. *Chem. Mater.* **1994**, *6*, 216–219.

7 Zhu, R.; Min, G.; Wei, Y.; Schmitt, H. J. Scanning Tunneling Microscopy and UV–Visible Spectroscopy Studies of Lead Sulfide Ultrafine Particles Synthesized in Langmuir–Blodgett Films. *J. Phys. Chem.* **1992**, *96*, 8210–8211.

8 Guo, Q.; Teng, X.; Rahman, S.; Yang, H. Patterned Langmuir–Blodgett Films of Monodisperse Nanoparticles of Iron Oxide Using Soft Lithography. *J. Am. Chem. Soc.* **2003**, *125*, 630–631.

9 Benjamin, I. Chemical Reactions and Solvation at Liquid Interfaces: A Microscopic Perspective. *Chem. Rev.* **1996**, *96*, 1449–1475.

10 Luo, G.; Malkova, S.; Yoon, J.; Schultz, D. G.; Lin, B.; Meron, M.; Benjamin, I.; Vanysek, P.; Schlossman, M. L. Ion-Distributions Near a Liquid-Liquid Interface. *Science* **2006**, *311*, 216–218.

11 Binder, W. H. Supramolecular Assembly of Nanoparticles at Liquid-Liquid Interfaces. *Angew. Chem., Int. Ed.* **2005**, *44*, 2–5.

12 Binks, B. P.; Clint, J. H. Solid Wettability from Surface Energy Components: Relevance to Pickering Emulsions. *Langmuir* **2002**, *18*, 1270–1273.

13 Lin, Y.; Skaff, H.; Emrick, T.; Dinsmore, A. D.; Russel, T. P. Nanoparticle Assembly and Transport at Liquid-Liquid Interfaces. *Science* **2003**, *299*, 226–229.

14 Benkoski, J.; Jones, R. L.; Doughlas, J. F.; Karim, A. Photocurable Oil/Water Interfaces as a Universal Platform for 2-D Self-Assembly. *Langmuir* **2007**, *23*, 3530–3537.

15 Brust, M.; Walker, M.; Bethell, D.; Schiffrin, D. J.; Whyman, R. Synthesis of Thiol-Derivatised Gold Nanoparticles in a Two-Phase Liquid-Liquid System. *J. Chem. Soc., Chem. Commun.* **1994**, 801–802.

16 Kleitz, F.; Marlow, F.; Stucky, G. D.; Schuth, F. Mesoporous Silica Fibers: Synthesis, Internal Structure, and Growth Kinetics. *Chem. Mater.* **2001**, *13*, 3587–3595.

17 Sathaye, S. D.; Patil, K. R.; Paranjape, D. V.; Mitra, A.; Awate, S. V.; Mandale, A. B. Preparation of Q-Cadmium Sulfide Ultrathin Films by a New Liquid—Liquid Interface Reaction Technique (LLRT). *Langmuir* **2000**, *16*, 3487–3490.

18 Pan, D.; Jiang, S.; An, L.; Jiang, B. Controllable Synthesis of Highly Luminescent and Monodisperse CdS Nanocrystals by a Two-Phase Approach under Mild Conditions. *Adv. Mater.* **2004**, *16*, 982–985.

19 Schwartz, H.; Harel, Y.; Efrima, S. Surface Behavior and Buckling of Silver Interfacial Colloid Films. *Langmuir* **2001**, *17*, 3884–3892.

20 Dai, L. L.; Sharma, R.; Wu, C. Self-Assembled Structure of Nanoparticles at a Liquid—Liquid Interface. *Langmuir* **2005**, *21*, 2641–2643.

21 Song, J. M.; Zhu, J. H.; Yu, S. H. Crystallization and Shape Evolution of Single-Crystalline Selenium Nanorods at Liquid—Liquid Interface: From Monodisperse Amorphous Se Nanospheres toward Se Nanorods. *J. Phys. Chem. B* **2006**, *110*, 23790–23795.

22 Foster, P. M.; Thomas, P. M.; Cheetham, A. K. Biphasic Solvothermal Synthesis: A New Approach for Hybrid Inorganic—Organic Materials. *Chem. Mater.* **2002**, *14*, 17–20.

23 (a) Rao, C. N. R.; Kulkarni, G. U.; Thomas, P. J.; Agrawal, V. V.; Saravanan, P. Films of Metal Nanocrystals Formed at Aqueous—Organic Interfaces. *J. Phys. Chem. B* **2003**, *107*, 7391–7395. (b) Rao, C. N. R.; Kulkarni, G. U.; Agrawal, V. V.; Gautam, U. K.; Ghosh, M.; Tumkurkar, U. Use of the Liquid-Liquid Interface for Generating Ultrathin Nanocrystalline Films of Metals, Chalcogenides, and Oxides. *J. Colloid Interface Sci.* **2005**, *289*, 305–318.

24 Agrawal, V. V.; Kulkarni, G. U.; Rao, C. N. R. Nature and Properties of Ultrathin Nanocrystalline Gold Films Formed at the Organic—Aqueous Interface. *J. Phys. Chem. B* **2005**, *109*, 7300–7305.

25 Agrawal, V. V.; Kulkarni, G. U.; Rao, C. N. R. Surfactant-Promoted Formation of Fractal and Dendritic Nanostructures of Gold and Silver at the Organic-Aqueous Interface. *J. Colloid Interface Sci.* **2008**, *318*, 501–506.

26 Agrawal, V. V.; Varghese, N.; Kulkarni, G. U.; Rao, C. N. R. Effects of the Change in Interparticle Distance Induced by Alkanethiols on the Optical Spectra and Other Properties of Nanocrystalline Gold Films. *Langmuir*, in press).

27 Agrawal, V. V.; Mahalakshmi, P.; Kulkarni, G. U.; Rao, C. N. R. Nanocrystalline Films of Au—Ag, Au—Cu, and Au—Ag—Cu Alloys Formed at the Organic—Aqueous Interface. *Langmuir* **2006**, *22*, 1846–1851.

28 Gautam, U. K.; Ghosh, M.; Rao, C. N. R. A Strategy for the Synthesis of Nanocrystal Films of Metal Chalcogenides and Oxides by Employing the Liquid-Liquid Interface. *Chem. Phys. Lett.* **2003**, *381*, 1–6.

29 Gautam, U. K.; Ghosh, M.; Rao, C. N. R. Template-Free Chemical Route to Ultrathin Single-Crystalline Films of CuS and CuO Employing the Liquid—Liquid Interface. *Langmuir* **2004**, *20*, 10776–10778.

30 Kalyanikutty, K. P.; Gautam, U. K.; Rao, C. N. R. Ultra-Thin Crystalline Films of ZnS and PbS Formed at the Organic—Aqueous Interface. *Solid State Sci.* **2006**, *8*, 296–302.

31 Kalyanikutty, K. P.; Gautam, U. K.; Rao, C. N. R. Ultra-Thin Crystalline Films of CdSe and CuSe Formed at the Organic—Aqueous Interface. *J. Nanosci. Nanotechnol.* **2007**, *7*, 1916–1922.

32 Sanyal, M. K.; Agrawal, V. V.; Bera, M. K.; Kalyanikutty, K. P.; Daillant, J.; Blot, C.; Kubowicz, S.; Konovalov, O.; Rao, C. N. R. Ordering of Gold Nanoparticles Formed at Liquid-Liquid Interface. *J. Phys. Chem. C*, in press.

33 Krishnaswamy, R.; Majumdar, S.; Ganapathy, R.; Agrawal, V. V.; Sood, A. K.; Rao, C. N. R. Interfacial Rheology of an Ultrathin Nanocrystalline Film Formed at the Liquid/Liquid Interface. *Langmuir* **2007**, *23*, 3084–3087.

34 Krishnaswamy, R.; Kalyanikutty, K. P.; Kanishka, B.; Sood, A. K.; Rao, C. N. R. Nonlinear Viscoelasticity of Ultrathin Nanocrystalline Semiconducting Films of CdS and CuS at Liquid-Liquid Interfaces. *J. Colloid Interface Sci.*, (submitted for publication).